

Cite this: *Chem. Sci.*, 2025, 16, 4450

All publication charges for this article have been paid for by the Royal Society of Chemistry

Received 23rd August 2024  
Accepted 15th January 2025

DOI: 10.1039/d4sc05663a

rsc.li/chemical-science

# A coordination polymer with a silylene-supported Pd<sub>6</sub> core as an efficient heterogeneous hydrogenation catalyst†

Taiga Mitomo,<sup>b</sup> Yoshimasa Wada,<sup>ab</sup> Tetsuro Suda,<sup>b</sup> Atsushi Tamura,<sup>a</sup> Shunsuke Yagi,<sup>a</sup> Soichi Kikkawa,<sup>c</sup> Seiji Yamazoe<sup>c</sup> and Yusuke Sunada<sup>\*ab</sup>

A hexanuclear palladium cluster supported by two silylene units was readily linked by molecules of a linear ditopic isocyanide to afford a coordination polymer that retained the core Pd<sub>6</sub>(SiPh<sub>2</sub>)<sub>2</sub>Cl<sub>2</sub> framework. The obtained coordination polymer exhibited good performance as a heterogeneous catalyst in the hydrogenation of various alkenes in common organic solvents and in protic solvents such as H<sub>2</sub>O. Furthermore, the obtained coordination polymer showed sufficient stability during the hydrogenation in order for it to be recycled and reused.

## Introduction

Heterogeneous catalysts such as metal nanoparticles immobilized on solid supports are fundamental materials in a wide range of fields in modern materials science.<sup>1</sup> For example, Pd/C, which is composed of Pd nanoparticles embedded on charcoal, serves as a good catalyst in various organic transformations.<sup>2</sup> Considering the superior catalytic performance of certain metal clusters such as Pd<sub>n</sub> clusters,<sup>3</sup> solid-supported metal clusters are another class of heterogeneous catalysts that have attracted attention.<sup>4</sup> More recently, coordination polymers with 2D or 3D network architectures consisting of molecular-based metal species as the core and bridging organic ligands as linkers have attracted increasing attention as heterogeneous catalysts. A typical example of such coordination polymers is metal–organic frameworks, which have been intensively investigated and applied as catalysts.<sup>5</sup> In these materials, the judicious selection of appropriate core metal-containing molecules and bridging organic linkers is crucial for developing effective catalyst systems.

Considering the superior catalytic performance of Pd(0) aggregates, the construction of coordination polymers by incorporating Pd species as the core can be envisaged as a straightforward approach to synthesizing effective

heterogeneous catalysts. However, this strategy remains scarcely explored.<sup>6</sup> In fact, McPherson, Pedersen, and coworkers have recently reported the only example of a coordination polymer consisting of Pd(0) cluster molecules, namely, a triangular Pd<sub>3</sub> cluster-based organometallic 2D-coordination polymer, which was synthesized *via* the reaction of trinuclear [Pd(CNXyl)<sub>2</sub>]<sub>3</sub> (Xyl = 2,6-Me<sub>2</sub>-C<sub>6</sub>H<sub>3</sub>) with a linear ditopic isocyanide. However, the obtained coordination polymer showed limited catalytic performance in the hydrogenation of styrene, with the conversion reaching only 5% when the reaction was performed at 40 °C for 4 h under 1 atm of H<sub>2</sub> with 0.5 mol% catalyst loading.<sup>7</sup> Thus, a more sophisticated strategy to construct Pd-based coordination polymers as catalysts needs to be established.

We have recently focused on the synthesis of Pd-based cluster molecules supported by organosilicon ligands and their application as catalysts.<sup>8,9</sup> For instance, a planar tetranuclear Pd cluster that functioned as an effective homogeneous catalyst in the hydrogenation of various alkenes was synthesized *via* the reaction of [Pd(CN<sup>t</sup>Bu)<sub>2</sub>]<sub>3</sub> with a cyclic tetrasilane (Si<sub>4</sub>R<sub>8</sub>; R = <sup>i</sup>Pr, cyclopentyl).<sup>9a</sup> Motivated by the high catalytic performance of silylene-bridged Pd clusters, we planned to develop a heterogeneous catalyst by linking organosilicon-supported Pd clusters with appropriate bridging linkers to construct structurally rigid 3D coordination polymers. Herein, we wish to report the facile synthesis of a coordination polymer by linking a silylene-supported Pd<sub>6</sub> cluster having an edge-sharing tetrahedron framework with a linear ditopic isocyanide and its application as a heterogeneous catalyst in the hydrogenation of alkenes. A characteristic feature of this catalyst system is that it was effective in common organic solvents and protic solvents such as H<sub>2</sub>O, enabling the hydrogenation of alkenes bearing polar substituents such as –SO<sub>3</sub><sup>−</sup> and –B(OH)<sub>2</sub>. Furthermore, the high stability of the framework structure of

<sup>a</sup>Department of Applied Chemistry, School of Engineering, The University of Tokyo, 4-6-1, Komaba, Meguro-ku, Tokyo 153-8505, Japan

<sup>b</sup>Institute of Industrial Science, The University of Tokyo, 4-6-1, Komaba, Meguro-ku, Tokyo 153-8505, Japan

<sup>c</sup>Department of Chemistry, Graduate School of Science, Tokyo Metropolitan University, 1-1 Minami-Osawa, Hachioji, Tokyo, 192-0397, Japan

† Electronic supplementary information (ESI) available: Experimental, crystallographic details, and crystal data for 2. CCDC 2375542. For ESI and crystallographic data in CIF or other electronic format see DOI: <https://doi.org/10.1039/d4sc05663a>



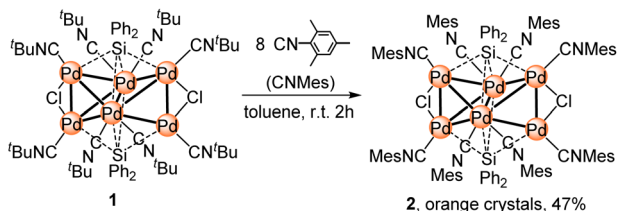
the heterogeneous catalyst even during the reaction in H<sub>2</sub>O allowed it to be recycled and reused.

## Results and discussion

### Ligand exchange reaction of silylene-supported Pd<sub>6</sub> cluster 1

Hexanuclear Pd cluster **1** was selected as the building block of the coordination polymer because the six Pd atoms in **1** are arranged into a 3D-shaped edge-sharing tetrahedron architecture.<sup>10</sup> First, ligand-exchange reactions involving the eight CN<sup>t</sup>Bu ligands in **1** were examined; however, no reaction occurred between **1** and 8 equiv. of nitrogen-containing ligands such as pyridine, 4,4'-bipyridine, and 1,4-diazabicyclo[2.2.2]octane at room temperature. In addition, complete decomposition of **1** was observed during the reaction of **1** with 8 equiv. of PMe<sub>2</sub>Ph or N-heterocyclic carbene <sup>i</sup>PrIM<sup>Me</sup> (<sup>i</sup>PrIM<sup>Me</sup> = 1,3-diisopropyl-4,5-dimethylimidazol-2-ylidene) at room temperature. In contrast, the ligand-exchange reaction between **1** and 8 equiv. of CNMes (Mes = 2,4,6-Me<sub>3</sub>-C<sub>6</sub>H<sub>2</sub>) readily proceeded in toluene at room temperature to afford cluster **2** in 47% isolated yield after 2 h of reaction (Scheme 1).

Although the data are not sufficient with an R<sub>1</sub> value of 8.69%, presumably due to the small and low quality of the obtained crystals, the molecular structure of **2** was determined by an X-ray diffraction (XRD) analysis (Fig. 1). Consistent with the solid-state structure, the <sup>1</sup>H spectrum of **2** at room temperature showed four singlets assignable to the methyl groups on the mesityl group of CNMes at 1.82, 1.93, 2.06, and 2.38 ppm with an integral ratio of 12 : 12 : 24 : 24 (Fig. S20<sup>†</sup>). The <sup>13</sup>C NMR



Scheme 1 Synthesis of **2**.

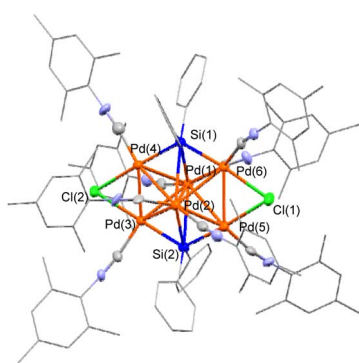


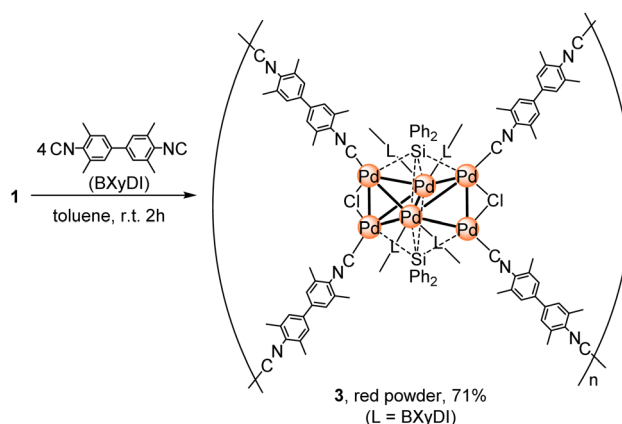
Fig. 1 Molecular structure of **2** with thermal ellipsoids at 50% probability. All carbon atoms except for those in the coordinated -CN moieties are shown in wireframe style, and all hydrogen atoms are omitted for clarity.

signals derived from the methyl groups of the mesityl groups appeared at 18.77, 19.24, 20.74 and 20.90 ppm (Fig. S21<sup>†</sup>). In the <sup>29</sup>Si NMR spectrum, a singlet appeared at 104.70 ppm, which is slightly shifted to a lower field compared to that of **1** (98.8 ppm) (Fig. S22<sup>†</sup>). In the infrared (IR) spectrum, two strong absorption bands derived from the C≡N bond were observed at 2054 and 2104 cm<sup>-1</sup> (Fig. S23<sup>†</sup>). The elemental analysis of **2** was consistent with the theoretical values.

### Construction of coordination polymer **3** via the ligand-exchange reaction between **1** and a linear ditopic aryl isocyanide

Having demonstrated that **1** undergoes ligand-exchange reactions with aryl isocyanides, we selected a linear ditopic aryl isocyanide, *i.e.*, 3,3',5,5'-tetramethyl biphenyl-4,4'-bisocyanide (BXYDI), as the bridging linker to construct a coordination polymer based on the Pd<sub>6</sub> cluster framework. Treatment of **1** with 4 equiv. of BXYDI in toluene at room temperature for 2 h furnished **3** as a red powder in 71% yield. Unfortunately, several attempts to obtain single crystals of **3** were unsuccessful, which prevented the determination of the molecular structure of **3** by a single crystal XRD analysis.

Compound **3** is insoluble in organic solvents including THF, toluene, Et<sub>2</sub>O, pentane, CH<sub>3</sub>CN, EtOH, and MeOH as well as in H<sub>2</sub>O. Its elemental analysis was consistent with the theoretical value calculated for the coordination polymer consisting of a Pd<sub>6</sub>(SiPh<sub>2</sub>)<sub>2</sub>Cl<sub>2</sub> core unit supported by eight surrounding BXYDI ligands (Scheme 2). In other words, two central Pd atoms are connected to two isocyanide ligands, and each of the four Pd atoms located on the edge bears one BXYDI ligand. In addition, an X-ray fluorescence (XRF) microanalysis of a powder sample of **3** indicated that the Pd : Si : Cl molar ratio was 29.90 : 3.44 : 2.36, which agrees well with the theoretical value (Pd : Si : Cl = 30.18 : 3.35 : 2.66). To gain further insight into the structure and electronic state of **3**, an X-ray photoelectron-spectroscopy (XPS) analysis of **1–3** was performed (Fig. S12–S17<sup>†</sup>). First, the elemental composition of **3** was estimated to be Pd : Cl : N = 6 : 2.05 : 7.94, which is consistent with the formula shown in



Scheme 2 Synthesis of **3** via the reaction of **1** with linear ditopic aryl isocyanide BXYDI.



Scheme 2. The XPS spectrum of **1** and **2** showed Pd 3d<sub>5/2</sub> signals at 335.8 eV for **1** and 336.1 eV for **2**, respectively. Because these signals could not be deconvoluted, the oxidation state of all palladium atoms in **1** and **2** could be considered identical due to the electronic delocalization. Clusters **1** and **2** consist of six palladium atoms surrounded by two silylenes, eight isocyanides, and two chloride ligands. Among them, both silylene<sup>11</sup> and isocyanide could be regarded as neutral ligands, and thus, the oxidation state of the Pd<sub>6</sub> core could be regarded as +2. The Pd 3d<sub>5/2</sub> signals in **1** (335.8 eV) and **2** (336.1 eV) are located in the region between the signal for Pd(0) metal (335.2 eV)<sup>12</sup> and that of palladium(II) oxide (337.1 eV).<sup>13</sup> These spectral features agree well with the slightly electron deficient nature of Pd atoms in **1** and **2** compared with the Pd(0) oxidation state.

The XPS spectrum of **3** showed Pd 3d signals at 335.20 eV (3d<sub>5/2</sub>) and 340.52 eV (3d<sub>3/2</sub>), which are slightly shifted to lower energies compared with those of the parent cluster **1** (335.8 and 340.9 eV). This result suggests that the Pd center in **3** might be slightly electron rich compared with **1**, but the electronic environment around Pd atoms is almost maintained upon the formation of the coordination polymer. It should be noted here that the Pd(0) center in a recently reported silylyne-bridged tetranuclear Pd cluster (335.8 and 340.8 eV).<sup>14</sup> In the IR spectrum of **3**, a relatively broad absorption band derived from the coordinated BXYDI appeared at around 2064 and 2095 cm<sup>-1</sup>.

Subsequently, **1** and **3** were subjected to a Pd K-edge X-ray absorption spectroscopy (XAS) analysis to obtain more insight into the structure of **3**. It should be emphasized here that the XANES spectrum of a powder sample of **3** was almost identical to that of a powder sample of **1**, indicating that the solid-state structure and electronic state of the Pd<sub>6</sub> cluster core were maintained in **3**. A curve-fitting analysis of the Pd K-edge Fourier transform extended X-ray absorption fine structure (FT-EXAFS) spectrum of **1** revealed that each of the Pd atoms is bound to adjacent Pd, Si, and Cl atoms with Pd–Pd, Pd–Si, Pd–Cl, and Pd–C (isocyanide) bond distances of *ca.* 2.78, 2.33, 2.50, and 1.96 Å, respectively (Table 1). The coordination numbers (CNs) of the Pd–Pd, Pd–Si, Pd–Cl, and Pd–C interactions were determined to be *ca.* 2.7, 0.9, 0.8, and 1.0, respectively. These bond distances and CNs are in accordance with those of the single-crystal XRD structure of **1**.<sup>8</sup> Based on the FT-EXAFS spectrum of **3**, the Pd–Pd, Pd–Si, and Pd–C bond distances

were estimated to be 2.74, 2.52, and 2.00 Å, and the CNs for Pd–Pd, Pd–Si, and Pd–C were *ca.* 3.1, 0.5, and 1.1 (Table 1). The estimated Pd–Pd and Pd–C bond distances are in good agreement with those estimated based on the FT-EXAFS spectrum of **1**. In contrast, the Pd–Si bond in **3** is relatively longer than that in **1**, and no apparent Pd–Cl bonding interaction was observed. Instead, the CN of Pd–Pd increased and that of Pd–Si decreased upon the formation of coordination polymer **3**. Considering the results of the XRF, XPS, and elemental analyses, which indicate the presence of Cl atoms in **3** in a Pd:Cl ratio of 6:2 (*vide supra*), the XAFS results suggest that the disappearance of the Pd–Cl bond and the change in the CN value of the Pd–Pd and Pd–Si bonds in **3** might stem from the slightly shrunken hexapalladium-cluster-framework core with relatively weakened Pd–Cl and Pd–Si bonds. Considering these results, we concluded that **3** is composed of a Pd<sub>6</sub>(SiPh<sub>2</sub>)<sub>2</sub>Cl<sub>2</sub> core architecture similar to cluster molecule **2** and that this core unit is linked by molecules of the linear ditopic isocyanide BXYDI.

Unfortunately, several attempts to obtain single crystals of **3** suitable for single crystal X-ray diffraction analysis were unsuccessful. Thus, a powder X-ray diffraction analysis of **1** and **3** was performed. The powder X-ray diffraction pattern of **1** might be comparable to the simulated pattern, which was estimated from a molecular structure determined by a single crystal X-ray diffraction analysis, but it is difficult to draw conclusions due to the low signal to noise ratio of the experimental diffractogram (Fig. S18†). In contrast, powder X-ray diffraction analysis of **3** showed only background noise and a halo pattern, suggesting that **3** was obtained as an amorphous material.

### Catalytic hydrogenation of alkenes mediated by coordination polymer **3**

As **3** was obtained as an insoluble powder, we turned our attention to its potential use as a heterogeneous catalyst for the hydrogenation of alkenes. For that purpose, the catalytic performance of **3** was initially examined in the hydrogenation of styrene, which revealed that the reaction completed within 6 h under 1 atm of H<sub>2</sub> at room temperature in toluene in the presence of 2 mol% (for Pd) of **3** to afford ethylbenzene as the single product (Table 2, entry 2). Similarly, the hydrogenation of 9-vinylanthracene also resulted in complete conversion of the

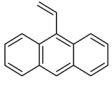
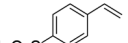
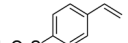
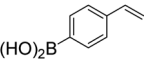
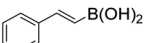
Table 1 Structural parameters of **1**, **3** (as prepared) and **3** (recycled) obtained by curve fitting analysis of Pd K-edge FT-EXAFS<sup>a</sup>

Compound	Atom	Coordination number	Bond length (Å)	Debye–Waller factor	R factor (%) <sup>a</sup>
<b>1</b>	C	1.0 ± 0.3	1.96 ± 0.07	0.005 ± 0.004	13.9
	Si	0.9 ± 0.2	2.33 ± 0.05	0.004 ± 0.001	
	Cl	0.8 ± 0.2	2.50 ± 0.08	0.006 ± 0.005	
	Pd	2.7 ± 0.3	2.78 ± 0.04	0.010 ± 0.005	
<b>3</b> (as prepared)	C	1.1 ± 0.3	2.00 ± 0.06	0.003 ± 0.002	12.9
	Si	0.5 ± 0.4	2.52 ± 0.12	0.027 ± 0.026	
	Pd	3.1 ± 0.4	2.74 ± 0.05	0.014 ± 0.014	
<b>3</b> (recycled)	C	0.8 ± 0.3	1.99 ± 0.07	0.003 ± 0.003	14.8
	Si	0.4 ± 0.2	2.46 ± 0.10	0.009 ± 0.008	
	Pd	2.5 ± 0.3	2.73 ± 0.04	0.010 ± 0.006	

$$^a R = (\sum(k^3 \chi^{\text{data}}(k) - k^3 \chi^{\text{fit}}(k))^2)^{1/2} / (\sum(k^3 \chi^{\text{data}}(k))^2)^{1/2}.$$



Table 2 Hydrogenation of alkenes catalyzed by **1** or **3**<sup>a</sup>

Entry	Cat.	Time (h)	Solvent	Alkene	Yield (%) <sup>b</sup>
$\text{R}-\text{CH}=\text{CH}_2 + \text{H}_2 \xrightarrow[\text{solvent, r.t., time}]{\text{cat. 1 or 3 (2 mol\% for Pd), (1 atm)}} \text{R}-\text{CH}_2-\text{CH}_2-\text{H}$					
1	<b>1</b>	18	Toluene		20 <sup>c</sup>
2	<b>3</b>	6	Toluene		>99
3	Pd/C	6	Toluene		>99
4	<b>1</b>	6	H <sub>2</sub> O		25 <sup>c</sup>
5	<b>3</b>	6	H <sub>2</sub> O		>99
6	Pd/C	6	H <sub>2</sub> O		21
7	<b>3</b>	18	Toluene		>99
8	<b>1</b>	18	H <sub>2</sub> O		10 <sup>c</sup>
9	<b>3</b>	18	H <sub>2</sub> O		>99 (92) <sup>d</sup>
10	<b>3</b>	18	CH <sub>3</sub> OH		>99 (80) <sup>d</sup>
11	<b>3</b>	18	CH <sub>3</sub> OH		>99 (72) <sup>d</sup>

<sup>a</sup> All reactions were carried out using 1 mmol of alkene in the presence of a catalytic amount of catalyst **1**, **3** or Pd/C in the solvent indicated in Table 1 (2 mL). The catalyst loading of 2 mol% indicates the total catalyst loading of Pd (0.02 mmol of Pd) in all experiments. <sup>b</sup> The product yield was determined by <sup>1</sup>H NMR spectroscopy in the presence of 1,4-dioxane as the internal standard, which was used to determine the conversion of the starting material. <sup>c</sup> The formation of a black insoluble material was observed. <sup>d</sup> Values in parentheses refer to the isolated yield.

substrate (entry 7). In contrast, the conversion of styrene reached only 20% when the reaction was conducted with 2 mol% (for Pd) of **1** (entry 1). During the reaction mediated by **1**, a black insoluble material was formed after 18 h, suggesting that decomposition of **1** occurred. Conversely, **3** was sufficiently stable under the applied hydrogenation conditions, and no dissolved BXyDI linker was observed in the <sup>1</sup>H NMR spectra of the reaction mixture.

The hydrogenation of alkenes catalyzed by the conventional Pd/C catalyst is generally conducted in organic solvents or alcohols. However, the development of organic reactions performed in H<sub>2</sub>O has recently received much attention because H<sub>2</sub>O is a safe, nonflammable, inexhaustible, and naturally abundant solvent.<sup>15</sup> Interestingly, **3** could be used in protic solvents such as H<sub>2</sub>O and MeOH. For instance, styrene underwent complete hydrogenation in H<sub>2</sub>O under atmospheric pressure of H<sub>2</sub> at room temperature catalyzed by **3** (entry 4), whereas the immediate decomposition of **1** occurred under the same reaction conditions, affording the product in only 25% yield (entry 5). It is noteworthy that hydrogenation of styrene catalyzed by conventional Pd/C in H<sub>2</sub>O gave the product only in 21% yield (entry 6). This indicates that coordination polymer catalyst **3** showed superior catalytic performance to the conventional Pd catalyst in the reaction performed in H<sub>2</sub>O.

Next, we focused on the use of *p*-styrenesulfonic acid sodium salt as the substrate given that it shows limited solubility in common organic solvents but good solubility in H<sub>2</sub>O. It should be noted here that the hydrogenation of *p*-styrenesulfonic acid sodium salt in H<sub>2</sub>O has been reported to be difficult, even when using a water-soluble cationic Ru catalyst.<sup>16</sup> The effective hydrogenation of this substrate has only been achieved using a Rh complex sorbed on the aluminophosphate molecular sieve VPI-5 (ref. 17) or a water-soluble polymer-bound metal catalyst.<sup>18</sup> Nevertheless, treatment of *p*-styrenesulfonic acid sodium salt with 2 mol% of **3** in H<sub>2</sub>O at room temperature for 18 h furnished the hydrogenated product quantitatively in 92% isolated yield (entry 9). In stark contrast, the hydrogenated product was obtained in a low 10% yield under identical reaction conditions mediated by **1** (entry 8), most likely due to the high moisture sensitivity of **1**. In addition, we confirmed that the catalysis mediated by **3** was applicable to the hydrogenation of alkenes bearing a -B(OH)<sub>2</sub> group. Thus, the hydrogenation of 4-vinyl phenyl boronic acid and *trans*-2-phenyl boronic acid was realized in MeOH under 1 atm of H<sub>2</sub> at room temperature (entries 10 and 11), and the corresponding products were isolated in 80% and 72% yields, respectively. These results indicate that **3** can be used in reactions conducted in both organic and protic solvents.

Interestingly, we discovered that catalyst **3** can be recycled multiple times in the hydrogenation of *p*-styrenesulfonic acid sodium salt (for details, see the ESI†). The first run of the catalytic hydrogenation was performed under 1 atm of H<sub>2</sub> in H<sub>2</sub>O at room temperature for 18 h in the presence of 2 mol% (for Pd) of **3**. Subsequently, the reaction mixture was centrifuged and catalyst **3** was recovered and subjected to the next run of the same hydrogenation process. After four cycles, the recovered catalyst retained high catalytic activity, and the desired product was obtained in quantitative yield in all runs. Thus, **3** could be reused at least four times by centrifugation without significant loss of the catalytic performance.

To gain further insight into the stability of the structure of **3**, the red powder of **3** recovered after one cycle of the hydrogenation of *p*-styrenesulfonic acid sodium salt under the conditions shown in entry 9, Table 2 was subjected to an XAS analysis. A comparison of the XANES spectra (Fig. S10†) revealed that the spectrum of the recovered catalyst was roughly identical to that of fresh **3**. Based on the FT-EXAFS spectrum of the recovered catalyst, the Pd-Pd, Pd-Si, and Pd-C (isocyanide) bond distances were estimated to be *ca.* 2.73, 2.46, and 1.99 Å, respectively, and the CNs for Pd-Pd, Pd-Si, and Pd-C were 2.5, 0.4, and 0.8 (Table 1). It is important to note here that the signal of the Pd-Pd bond was not enhanced compared with that of fresh **3**, indicating that no aggregation of Pd atoms to form Pd nanoparticles occurred. These spectral results suggest that the structure of **3** consisting of a Pd<sub>6</sub>(SiPh<sub>2</sub>)<sub>2</sub>Cl<sub>2</sub> core unit linked by linear ditopic BXyDI ligands remains stable during the catalysis.

## Conclusions

We have discovered that a hexanuclear Pd cluster supported by two silylene SiPh<sub>2</sub> units can be readily linked by molecules of



a linear ditopic isocyanide to afford coordination polymer **3**, which can serve as a heterogeneous catalyst for the hydrogenation of alkenes with excellent catalytic activity. Interestingly, the catalysis could be performed in common organic solvents and in H<sub>2</sub>O, which allows the hydrogenation of water-soluble alkenes. Catalyst **3** exhibited sufficient stability under the applied reaction conditions and can be recycled and reused at least four times. X-ray fluorescence (XRF), X-ray absorption fine structure (XAFS), and elemental analyses revealed that **3** consists of a Pd<sub>6</sub>(SiPh<sub>2</sub>)<sub>2</sub>Cl<sub>2</sub> core linked by linear ditopic isocyanide ligands and that the Pd cluster framework was retained during the catalytic hydrogenation in H<sub>2</sub>O. The results of this study suggest that linking silicon-bridged metal clusters provides an effective strategy to construct coordination polymers that can serve as heterogeneous catalysts with high catalytic performance and durability.

## Data availability

All experimental data are provided in the ESI.†

## Author contributions

T. M. carried out the synthesis, characterization, and catalysis. Y. W. and T. S. helped with the XPS measurements and their analysis. Y. S. conceptualized and supervised the project. A. T. and S. Y. performed the powder XRD measurements. S. K. and S. Y. performed the XAS measurements. The manuscript was written through contributions of all authors. All authors have approved the final version of the manuscript.

## Conflicts of interest

The authors declare no competing financial interest.

## Acknowledgements

This work was supported by JST (Japan) in the form of the PRESTO grant JPMJPR20A9 and JSPS KAKENHI Grant Numbers JP24K01495. The synchrotron radiation experiments were performed at the BL01B1 of SPring-8 with the approval of the Japan Synchrotron Radiation Research Institute (JASRI) (Proposal No. 2022B1259).

## References

- (a) S. Navalon, A. Dhakshinamoorthy, M. Alvaro and H. Garcia, *Coord. Chem. Rev.*, 2016, **312**, 99–148; (b) R. J. White, R. Luque, V. L. Budarin, J. H. Clark and D. J. Macquarrie, *Chem. Soc. Rev.*, 2009, **38**, 481–494; (c) J. M. Campelo, D. Luna, R. Luque, J. M. Marinas and A. A. Romero, *ChemSusChem*, 2009, **2**, 18–45; (d) M. J. Ndolomingo, N. Bingwa and R. Meijboom, *J. Mater. Sci.*, 2020, **55**, 6195–6241; (e) A. Fukuoka and P. L. Dhepe, *Chem. Rec.*, 2009, **9**, 224–235.
- (a) A. Bavykina, N. Kolobov, I. S. Khan, J. A. Bau, A. Ramirez and J. Gascon, *Chem. Rev.*, 2020, **120**, 8468–8535; (b) J. Liu, L. Chen, H. Cui, J. Zhang, L. Zhang and C.-Y. Su, *Chem. Soc. Rev.*, 2014, **43**, 6011–6061; (c) A. Corma, H. Garcia and F. X. Llabrés i Xamena, *Chem. Rev.*, 2010, **110**, 4606–4655; (d) Y.-B. Huang, J. Liang, X.-S. Wang and R. Cao, *Chem. Soc. Rev.*, 2017, **46**, 126–157; (e) J. Gascon, A. Corma, F. Kapteijn and F. X. Llabrés i Xamena, *ACS Catal.*, 2014, **4**, 361–378; (f) J. Guo, Y. Qin, Y. Zhu, X. Zhang, C. Long, M. Zhao and Z. Tang, *Chem. Soc. Rev.*, 2021, **50**, 5366–5396; (g) N. F. Suremann, B. D. McCarthy, W. Gschwind, A. Kumar, B. A. Johnson, L. Hammarström and S. Ott, *Chem. Rev.*, 2023, **123**, 6545–6611; (h) Q. Wang and D. Astruc, *Chem. Rev.*, 2020, **120**, 1438–1511; (i) D. Yang and B. C. Gates, *ACS Catal.*, 2019, **9**, 1779–1798; (j) M. Yoon, R. Srirambalaji and K. Kim, *Chem. Rev.*, 2012, **112**, 1196–1231; (k) L. Zhu, X.-Q. Liu, H.-L. Jiang and L.-B. Sun, *Chem. Rev.*, 2017, **117**, 8129–8176; (l) J. Fonseca, T. Gong, L. Jiao and H.-L. Jiang, *J. Mater. Chem. A*, 2021, **9**, 10562–10611; (m) Z. Lin, J. J. Richardson, J. Zhou and F. Caruso, *Nat. Rev.*, 2023, **7**, 273–286; (n) J. Zhang and C.-Y. Su, *Coord. Chem. Rev.*, 2013, **257**, 1373–1408; (o) P. Sutar and T. K. Maji, *Chem. Commun.*, 2016, **52**, 8055–8074.
- (a) N. Jeddi, N. W. J. Scott and I. J. S. Fairlamb, *ACS Catal.*, 2022, **12**, 11615–11638; (b) N. Jeddi, N. W. J. Scott, T. Tanner, S. K. Beaumont and I. J. S. Fairlamb, *Chem. Sci.*, 2024, **15**, 2763–2777.
- (a) B. C. Gates, *Chem. Rev.*, 1995, **95**, 511–522; (b) B. C. Gates, Metal cluster catalysts dispersed on solid supports, in *Catalysis by Di- and Polynuclear Metal Cluster Complexes*, ed. R. D. Adams and F. A. Cotton, Wiley-VCH, New York, 1998, pp. 509–538; (c) S. Hermans, Clusters and Immobilization, in *Synthesis of Solid Catalysts*, ed. K. P. de Jong, Wiley-VCH, Weinheim, 2009, pp. 153–169; (d) H. Rong, S. Ji, J. Zhang, D. Wang and Y. Li, *Nat. Commun.*, 2020, **11**, 5884; (e) B. C. Gates, *J. Mol. Catal. A: Chem.*, 2000, **163**, 55–65; (f) J. Fang, B. Zhang, Q. Yao, Y. Yang, J. Xie and N. Yan, *Coord. Chem. Rev.*, 2016, **322**, 1–29; (g) Y. Du, H. Sheng, D. Astruc and M. Zhu, *Chem. Rev.*, 2019, **120**, 526–622; (h) C. Dong, Y. Li, D. Cheng, M. Zhang, J. Liu, Y.-G. Wang, D. Xiao and D. Ma, *ACS Catal.*, 2020, **10**, 11011–11045; (i) A. Kulkarni, R. J. Lobo-Lapidus and B. C. Gates, *Chem. Commun.*, 2010, **46**, 5997–6015.
- (a) J. G. de Vries and C. J. Elsevier, in *Handbook of Homogeneous Hydrogenation*, Wiley-VCH, Weinheim, 2007; (b) S. Nishimura, in *Handbook of Heterogeneous Catalytic Hydrogenation for Organic Synthesis*, Wiley-VCH, New York, 2001; (c) H.-U. Blaser, A. Indolese, A. Schnyder, H. Steiner and M. Studer, *J. Mol. Catal. A: Chem.*, 2001, **173**, 3–18; (d) X. Liu and D. Astruc, *Adv. Synth. Catal.*, 2018, **360**, 3426–3459; (e) F.-X. Felpin, *Synlett*, 2014, **25**, 1055–1067.
- (a) T. He, X.-J. Kong, J. Zhou, C. Zhao, K. Wang, X.-Q. Wu, X.-L. Lv, G.-R. Si, J.-R. Li and Z.-R. Nie, *J. Am. Chem. Soc.*, 2021, **143**, 9901–9911; (b) M. T. Payne, C. N. Neumann, E. Stavitski and M. Dincă, *Inorg. Chem.*, 2021, **60**, 11764–11774; (c) W. Zhang, Z. Chen, M. Al-Naji, P. Guo, S. Cwik, O. Halbherr, Y. Wang, M. Muhler, N. Wilde, R. Gläser and R. A. Fischer, *Dalton Trans.*, 2016, **45**, 14883–14887; (d)



- C.-H. Wang, W.-Y. Gao, Q. Ma and D. C. Powers, *Chem. Sci.*, 2019, **10**, 1823–1830; (e) Y. Dong, J.-J. Jv, X.-W. Wu, J.-L. Kan, T. Lin and Y.-B. Dong, *Chem. Commun.*, 2019, **55**, 14414–14417; (f) S. Parshamoni, R. Nasani, A. Paul and S. Konar, *Inorg. Chem. Front.*, 2021, **8**, 693–699; (g) J. A. Navarro, E. Barea, J. M. Salas, N. Masciocchi, S. Galli, A. Sironi, C. O. Ania and J. B. Parra, *Inorg. Chem.*, 2006, **45**, 2397–2399; (h) F. X. Llabrés i Xamena, A. Abad, A. Corma and H. Garcia, *J. Catal.*, 2007, **250**, 294–298.
- 7 X. Liu, J. N. McPherson, C. E. Andersen, M. S. Jørgensen, R. W. Larsen, N. J. Yutronkie, F. Wilhelm, A. Rogalev, M. Giménez-Marqués, G. M. Espallargas, C. R. Göb and K. S. Pedersen, *Nat. Commun.*, 2024, **15**, 1177.
- 8 Y. Sunada, K. Yamaguchi and K. Suzuki, *Coord. Chem. Rev.*, 2022, **469**, 214673.
- 9 (a) C. Yanagisawa, S. Yamazoe and Y. Sunada, *ChemCatChem*, 2021, **13**, 169–173; (b) K. Shimamoto and Y. Sunada, *Chem. Sci.*, 2022, **13**, 4115–4121; (c) R. Usui and Y. Sunada, *Inorg. Chem.*, 2021, **60**, 15101–15105; (d) N. Kojima, M. Kato and Y. Sunada, *Chem. Sci.*, 2022, **13**, 7610–7615; (e) Y. Umehara, R. Usui, Y. Wada and Y. Sunada, *Commun. Chem.*, 2023, **6**, 93; (f) K. Shimamoto and Y. Sunada, *Chem. Commun.*, 2021, **57**, 7649–7652; (g) R. Usui and Y. Sunada, *Chem. Commun.*, 2020, **56**, 8464–8467; (h) Y. Sunada, N. Taniyama, K. Shimamoto, S. Kyushin and H. Nagashima, *Inorganics*, 2017, **5**, 84; (i) Y. Sunada, R. Haige, K. Otsuka, S. Kyushin and H. Nagashima, *Nat. Commun.*, 2013, **4**, 3014.
- 10 K. Shimamoto and Y. Sunada, *Chem.–Eur. J.*, 2019, **25**, 3761–3765.
- 11 (a) R. Waterman, P. G. Hayes and T. D. Tilley, *Acc. Chem. Res.*, 2007, **40**, 712–719; (b) Y. Tsuchido, R. Abe, M. Kamono, K. Tanaka, M. Tanabe and K. Osakada, *Bull. Chem. Soc. Jpn.*, 2018, **91**, 858–864; (c) K. Osakada, M. Tanabe and T. Tanase, *Angew. Chem., Int. Ed.*, 2000, **39**, 4053–4055; (d) C. Watanabe, T. Iwamoto, C. Kabuto and M. Kira, *Angew. Chem., Int. Ed.*, 2008, **47**, 5386–5389.
- 12 (a) M. Luo, Z. Zhao, Y. Zhang, Y. Sun, Y. Xing, F. Lv, Y. Yang, X. Zhang, S. Hwang, Y. Qin, J.-Y. Ma, F. Lin, D. Su, G. Lu and S. Guo, *Nature*, 2019, **574**, 81–85; (b) C. Li, Q. Yuan, B. Ni, T. He, S. Zhang, Y. Long, L. Gu and X. Wang, *Nat. Commun.*, 2018, **9**, 3702; (c) W. Jiao, C. Chen, W. You, J. Zhang, J. Liu and R. Che, *Small*, 2019, **15**, 1805032; (d) W. Si, Z. Yang, X. Hu, Q. Lv, X. Li, F. Zhao, J. Hea and C. Huang, *J. Mater. Chem. A*, 2021, **9**, 14507.
- 13 A. Tressaud, S. Khairoun, H. Touhara and N. Watanabe, *Z. Anorg. Allg. Chem.*, 1986, **540**, 291.
- 14 J. Sekiguchi, Y. Kazama, A. Ishii and N. Nakata, *Chem. Commun.*, 2023, **59**, 9844–9847.
- 15 (a) R. Breslow, *Acc. Chem. Res.*, 1991, **24**, 159–164; (b) M. Cortes-Clerget, J. Yu, J. R. A. Kincaid, P. Walde, F. Gallou and B. H. Lipshutz, *Chem. Sci.*, 2021, **12**, 4237–4266; (c) T. Kitanosono and S. Kobayashi, *Chem.–Eur. J.*, 2020, **26**, 9408–9429; (d) C.-J. Li, *Chem. Rev.*, 1993, **93**, 2023–2035; (e) T. Kitanosono, K. Masuda, P. Xu and S. Kobayashi, *Chem. Rev.*, 2018, **118**, 679–746; (f) N. A. Harry, S. Radhika, M. Neetha and G. Anilkumar, *ChemistrySelect*, 2019, **4**, 12337–12355; (g) U. M. Lindström, *Chem. Rev.*, 2002, **102**, 2751–2772.
- 16 P. Csabai and F. Joó, *Organometallics*, 2004, **23**, 5640–5643.
- 17 J. R. Anderson, E. M. Campi, W. R. Jackson and Z. P. Yang, *J. Mol. Catal. A:Chem.*, 1997, **116**, 109–115.
- 18 D. E. Bergbreiter and Y.-S. Liu, *Tetrahedron Lett.*, 1997, **38**, 3703–3706.

